arXiv:1401.3010v2 [cond-mat.mes-hall] 25 Nov 2014

Non-Majorana subgap states in two-dimensional topological insulator-superconductor hybrid structures

Hoi-Yin Hui, Jay D. Sau, and S. Das Sarma
Department of Physics, Condensed Matter Theory Center and Joint Quantum Institute, University of Maryland, College Park, Maryland 20742-4111, USA
(Dated: November 26, 2014)

Contrary to the widespread belief that Majorana zero-energy modes, existing as bound edge states in 2D topological insulator (TI)-superconductor (SC) hybrid structures, are unaffected by non-magnetic static disorder by virtue of time-reversal symmetry, we show that such a protection against disorder does not exist in realistic multi-channel TI/SC/ferromagnetic insulator (FI) sandwich structures of experimental relevance since the time-reversal symmetry is explicitly broken locally at the SC/FI interface where the end Majorana mode (MM) resides. We find that although the MM itself and the *bulk* topological superconducting phase inside the TI are indeed universally protected against disorder, extra fermionic subgap states are generically introduced at the TI edge due to the presence of the FI/SC interface as long as multiple edge channels are occupied. We discuss the important implications of our finding for the detection and manipulation of the edge MM in TI/SC/FI experimental systems of current interest.

PACS numbers: 74.78.-w, 03.65.Vf, 74.45.+c

Current interest [1–4] in the search for solid-state Majorana modes (MMs), i.e. zero-energy Majorana bound states inside a superconducting gap, has increased sharply following a series of experimental reports [5–10] claiming empirical evidence for the existence of MMs in semiconductor (SM) nanowires in proximity to superconductors (SCs) in the presence of an external magnetic field precisely as predicted in earlier theoretical publications [11–13]. Very recent MM-motivated experimental interest [14] has focused also on 2D (i.e. the so-called quantum spin Hall system) and 3D topological insulators (TIs) in proximity to ordinary s-wave SCs, where, in fact, the first theoretical proposals for the existence of MMs were originally made by Fu and Kane [15, 16], and then followed up by others [17]. One substantive advantage of the TI-based MM proposals over the SM-based proposals is that the explicit presence of time-reversal symmetry (TRS) in the TI/SC system makes the bulk topological SC phase in the TI and the associated MMs immune to static non-magnetic disorder arising from impurities and defects invariably present in the environment. By contrast, the SM/SC hybrid topological structures hosting MMs are unprotected from non-magnetic disorder in the environment [see Fig. 2(a) for an illustrative example in which the MM is destroyed by strong disorder] since time-reversal invariance must be explicitly broken [18] in the SM/SC sandwich structures in order to produce the MM-carrying topological phase. We emphasize, however, that both the TI/SC and the SM/SC systems are protected from elastic disorder residing in the bulk superconductor itself [19] which can have no effect on the proximity-induced topological superconductivity in the TI or the SM material – the protection (or not) for the TI (or SM) system that we are discussing here is specifically from the disorder residing at the interface or inside the bulk TI (or SM) material.

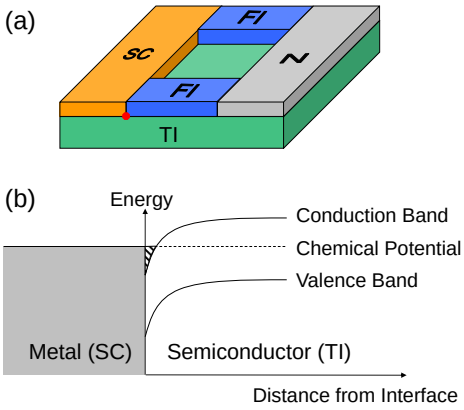

Figure 1. (a) Schematic picture of the devices: a TI in contact with SCs and an FI . The position of MM is marked with a red dot. The normal metal N acts as an external lead and the FI acts as a tunnel barrier. The MM is then detected as a zero-bias conductance peak. (b) At the interface between the metallic SC and the narrow-gap semiconductor (i.e. the TI), in general band-bending effect at the interface leads to extra edge channels (hashed region).

Although there have been many theoretical studies [20, 21] of disorder effects on the MMs and the topological superconductivity in the SM/SC nanowire systems of experimental relevance [5–10], including even some suggestions that the experimental observations of the zero bias peak [5–9] in the InSb and InAs semiconductor nanowires in the SM/SC hybrid structures, thought to be arising from the zero-energy bound MMs localized at the wire ends as predicted theoretically [11–13], are in fact direct manifestations of anti-localization effects induced by static disorder [22], there has been no theoretical analysis of disorder effects in the TI/SC hybrid structures

except for the work in Ref. [23] which concluded that TI/SC topological systems are completely protected from *all* elastic disorder effects by virtue of Anderson's theorem [24] due to TRS. A recent study, however, concluded that the induced p-wave superconductivity may in general be suppressed by disorder in a 3D TI/SC structure [25].

In the current work, we consider the experimental TI/SC structure for the existence of bound MMs where a ferromagnetic insulator (FI) must be deposited in order to localize the MMs at the system edge. The realistic structure [Fig. 1(a)], first proposed by Fu and Kane in this context [15], involves the 2D TI with SC and FI layers deposited on top of it, referred to as the STIM (superconductor-TI-magnet) system in Ref. [15]. The FI layer in the STIM breaks TRS which is essential for localizing spatially separated topologically non-Abelian MMs. The absolute necessity of TRS breaking for creating isolated defect-bound MMs is a well-established theorem [3].

In this scenario, the immunity of the local SC gap in the TI/SC/FI structure against disorder is subtle. Although Anderson's theorem guarantees that no impurities can degrade the gap deep in the SC region where TRS applies, there is no corresponding argument near the SC/FI interface where the FI provides an explicit TRS-breaking mechanism making the theorem inapplicable. This means that although the MMs separated by the SC do not hybridize, extra fermionic subgap states could potentially appear locally at the SC/FI interface in the TI/SC/FI hybrid structure. Our current work is the first theoretical exploration of the existence (or not) of such subgap states in STIM systems.

In spite of the explicit TRS-breaking, we find that disorder in the SC region of the TI edge is unable to generate any extra localized fermionic subgap states (i.e. in addition to the zero-energy MM itself) near the SC/FI interface [see Fig. 2(d)], provided that we limit our attention to only single-channel TI edges. Thus, the TI/SC/FI hybrid system is indeed immune to all disorder provided there is only a single active edge channel in the system. However, disorder-induced potential fluctuations near the edge are expected to produce bound states in addition to the 1D edge state. Such extra states or puddles, which have been proposed to explain the temperature dependence of the TI edge conductance [26], can be modeled using a multi-channel TI edge. In fact, in realistic structures, we expect multi-channel 1D edges in the generic 2D TI system due to, for example, band-bending effects which are ubiquitous near semiconductor surfaces.

We investigate a broad class of TI Hamiltonians by considering a multi-channel TI edge. In addition to disorder, the extra 1D edge channels could be induced from an intrinsically higher chemical potential near the surface [27, 28]. Also, since the 2D TI is commonly constructed from semiconductors with small band gaps (e.g. HgCdTe or InAs/GaSb) [29, 30], a proximate metallic SC would unavoidably induce extra edge channels due to band-bending [31] [see Fig. 1(b)].

We consider the following Hamiltonian which models a multi-channel TI edge in proximity to SC/FI:

$$
\begin{aligned}
H = \int dx \Bigg\{ & v \sum_{\alpha s s'} \left(\boldsymbol{p}_\alpha \cdot \boldsymbol{\sigma}_{ss'}\right) \psi^\dagger_{\alpha s}(x) \left(-i\partial_x\right) \psi_{\alpha s'}(x) \\
& - \sum_{\alpha\beta s} \mu_{\alpha\beta}(x) \psi^\dagger_{\alpha s}(x) \psi_{\beta s}(x) \\
& - \sum_{\alpha\beta i s s'} \tilde{\mu}^j_{\alpha\beta}(x) \imath \sigma^j_{ss'} \psi^\dagger_{\alpha s}(x) \psi_{\beta s'}(x) \\
& + \sum_\alpha \Delta_\alpha(x) \left[\psi_{\alpha\uparrow}(x)\psi_{\alpha\downarrow}(x) + \mathrm{hc}\right] \\
& + \sum_{\alpha s s'} B_\alpha(x) \sigma^x_{ss'} \psi^\dagger_{\alpha s}(x) \psi_{\alpha s'}(x) \Bigg\}
\end{aligned}
\tag{1}
$$

Here, $\psi^\dagger_{\alpha s}(x)$ creates an electron in the α^{th} channel with spin $s = \uparrow, \downarrow$ at position x, where each "channel" has a Kramers pair of bands. Note that the nature of TI edge requires the number of channels N_{ch} to be odd. $\boldsymbol{\sigma} = (\sigma^x, \sigma^y, \sigma^z)$ are the three Pauli spin matrices, and $\boldsymbol{p}_\alpha$ is the polarization of the α^{th} channel. The $N_{\text{ch}} \times N_{\text{ch}}$ real symmetric matrix $\mu_{\alpha\beta}(x)$ contains both the chemical potential of each channel (diagonal entries) and inter-channel elastic scattering (off-diagonal entries), while the anti-symmetric matrix $\tilde{\mu}^j_{\alpha\beta}(x)$ are the coefficients for inter-channel spin-orbit scatterings, which still respect TRS. The proximate SC and FI induce the local pairing potential $\Delta(x)$ and the Zeeman term $B(x)$ respectively. To model an SC/FI interface, we choose $\Delta(x) = \Delta\theta(x)$ and $B(x) = B\theta(-x)$ where $B = 3\Delta$, restricting the analysis to an idealized case where there are no spatial fluctuations of Δ and B on the edge [32] and no penetration of Δ and B to the FI and SC side respectively, since this would degrade the spectral gap at the SC/FI interface in a trivial way and obscure the main finding of this work. We also assume that there are no inter-channel pairings or Zeeman gaps.

Static charge impurities and spin-orbit impurities are included through spatial variations in $\mu(x)$ and $\tilde{\mu}(x)$ respectively. For the results below in which disorder is included, the mean free path l is estimated to be $k_F l \approx 3$. If the disorder in either μ or $\tilde{\mu}$ is removed, the phase space of scattering is reduced, but similar results would still apply provided that the mean free path remains the same by tuning up $\tilde{\mu}$ or μ respectively. Note that disorder is introduced in the SC region only since its effect on the FI region can in principle be offset by a sufficiently strong Zeeman term.

Before presenting the results based on numerical simulations, we first analyze the problem with a scattering matrix approach [20, 33], the details of which are presented in the Appendix. We treat the SC/FI in-

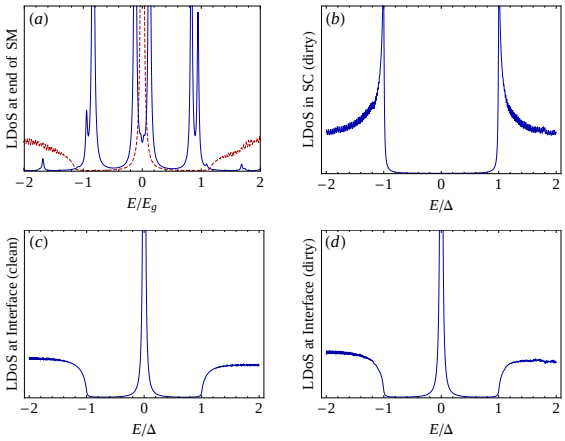

Figure 2. (a) LDOS at the end of a SM nanowire, where the dashed red line shows the result for a clean wire while the solid blue line is for a disordered wire. The parameters used for the BdG Hamiltonian $H = (\frac{p^2}{2m} + \alpha p\sigma_y - \mu)\tau_z + B\sigma_z + \Delta\tau_x$ are: $\mu = 0$, $B = 2\Delta$, $m\alpha^2 = 2\Delta$. (b) LDOS deep in the SC region of the TI edge, with disorder in SC region. (c) LDOS at the SC/FI interface on a clean TI. (d) LDOS at the SC/FI interface on a TI edge with disorder in SC region.

terface as an SC-N-FI system where the N region has a finite but vanishingly small width. Then, the localized modes at the interface are found by the condition $\det\left(1 - \tilde{R}R\right) = 0$ where $R(E)$ and $\tilde{R}(E)$ are respectively the reflection matrices at the SC-N and N-FI interfaces. At zero energy, R is constrained by unitarity, time-reversal symmetry, and particle-hole symmetry, while $\tilde{R}$ is constrained by unitarity and U(1) symmetry. From these constraints, we can show that $1 \le N_0 \le N_{\rm ch}$, where N_0 is the multiplicity of the unity eigenvalue of $\tilde{R}R$, which is equal to the number of localized zero-energy modes.

The exact value of N_0 depends on the details of the Hamiltonian, but one can always fine-tune the Hamiltonian near the SC/FI interface by local disorder respecting the symmetries, such that all energies of the localized modes reach zero. Therefore the constraint derived above implies that the number of localized states is equal to the number of channels in the TI edge, and among them there is always a zero-energy mode, which is the MM.

We have therefore shown that the gap protecting the MM is indeed robust in the single-channel case. This is not a consequence of Anderson's theorem as commonly believed, but is due to the various symmetries present in the system as elucidated by the above scattering matrix argument. Note that in the multi-channel case, although subgap states exist, the MM is still pinned at zero energy.

In the following we numerically study how the number of subgap states N_0 depends on the number of channels and other details of the interface.

We start by considering the simplest case of a TI/SC/FI interface where the TI has a single channel.

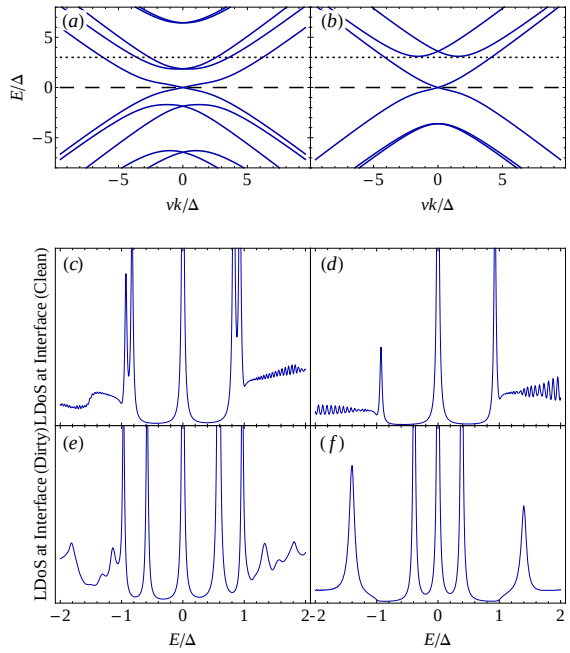

Figure 3. (a,b) Band structures of respectively a 5-channel and 3-channel TI edge. Here the parameters of Eq. (1) is chosen as: $\mu = \mathrm{diag}\,(2, -2, 1, -1, 0)\,\Delta$, $\tilde{\mu}^x = \tilde{\mu}^y = 0$, $\tilde{\mu}^z_{\alpha \gtrless \beta} = \pm 2\Delta$, $\boldsymbol{p}_\alpha = (+, -, +, -, +)\,\hat{z}$. The Fermi level in the FI region ($E_F = 0$) is shown in dashed line, while that in the SC region ($E_F = 3\Delta$) is shown in dotted line. (c,d) Their corresponding LDOS of at the SC/FI interface, without disorder. (e,f) Their corresponding LDOS at the SC/FI interface, with a single realization of non-magnetic disorder.

The local density of states (LDOS) [34] at the SC/FI interface with or without disorder is plotted respectively in Fig. 2(c,d). It shows that the LDOS in the subgap regime ($E < \Delta$) is not affected by disorder in the single-channel case. Fig. 2(b) shows that the gap deep in the SC region is also completely unaffected. This is consistent with previous results [23] and our scattering matrix analysis for the single-channel case. This simplification, however, disappears as soon as the system has multichannel edge states as is likely in realistic samples (Fig. 3).

To understand the interplay of disorder and multiple channels we consider 5-channel and 3-channel TI edge models. The parameters of Eq. (1) are so chosen so that the additional channels cross the Fermi level in the SC region. It is assumed that the FI region is gated so as to place the chemical potential in the gap of the additional bands as well [see Fig. 3(a,b)]. This is necessary to obtain localized MMs at the interface. The LDOS at the interface for several cases are plotted in Fig. 3(c,d,e,f). We typically find that each channel leads to a subgap state. The LDOS in Figs. 3(c,d) show that for the interface parameters chosen, the interface states are close to the edge of the gap away from the interface. On the other hand, introducing disorder leads to the results in Figs. 3(e,f), where one sees interface states that are bound deep inside

the bulk gap. The details of the SC/FI interface, such as the chemical potential change at the interface, can lead to scattering very similar to disorder effects. Therefore, depending on the details of the interface it is possible even for an interface without any explicit quenched disorder to have subgap states in the middle of the gap. The results plotted in Figs. 3(c,d) correspond to a smooth interface where such scattering is absent and therefore do not contain deep subgap states. In contrast to the interface LDOS, the LDOS in the SC region, away from the SC/FI interface, does not show any subgap states similar to the single channel case. This could be understood as a consequence of TRS, by which the application of Anderson's theorem forbids such subgap states.

Comparing the results of the disordered SC/FI interface in the single channel case (Fig. 2) and the multi-channel case (Fig 3) it is clear that the absence of subgap states in the single channel case is not simply a result of Anderson's theorem (i.e. TRS). As mentioned in the introduction, since TRS is locally broken at the interface, it only protects the bulk, i.e. the region away from the SC/FI interface, from subgap states. On the other hand, the scattering-matrix interpretation implies that the presence of a single subgap state in the single channel case is a result of the properties of the scattering matrix near zero energies. Time-reversal invariance does of course play a role in determining the properties of the scattering matrix. The scattering matrix picture also allows for the presence of extra subgap states in the multi-channel case as seen in Fig. 3.

The results in Fig. 3 are for a typical (rather than fine-tuned) structure of the interface (which is determined by the potentials in the various channels) and also for typical disorder configurations and should thus be regarded as typical results which should be qualitatively valid generically. While these results clearly establish the generic existence of fermionic subgap states in a multi-channel TI with disorder, the experimentally relevant question might be the likelihood of the occurrence of these subgap states with a random disorder potential. To address this question we calculate the disorder-averaged LDOS at the interface (Fig. 4). As seen from Fig. 4(a,b), the superconducting gap at the SC/FI interface is not protected against disorder and is reduced by increasing disorder strength. Interestingly, the disorder-averaged LDOS for strong disorder is found to vanish at zero energy. This suggests that level repulsion from the MM prevents the extra subgap states from approaching precise zero-energy which is consistent with conclusions from random matrix theory [35]. In Fig. 4(c,d) we show the disorder-averaged gap in the TI/SC edge away from the SC/FI interface. In contrast to the gap near SC/FI interface, we find that the TI/SC gap is immune to disorder as expected since TRS is respected there and Anderson's theorem applies. It is instructive to note that the LDOS at the interface [Fig. 4(a),(d)] shows precisely the same soft gap behavior

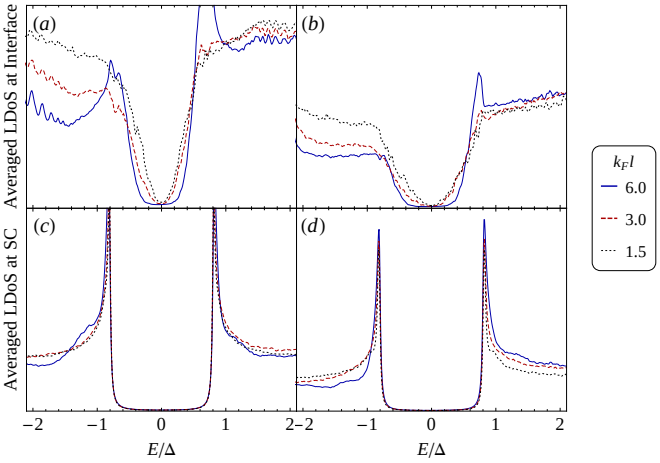

Figure 4. (a,b) LDOS at the SC/FI interface, averaged over 5000 realizations of non-magnetic disorder, for a 5-channel and 3-channel TI edge respectively. The three curves show the results for different strengths of disorder, and the MMs have been removed for clarity (c,d) Their corresponding averaged LDOS deep in the SC region.

widely observed in the SM/SC nanowire hybrid systems [32, 36].

The additional subgap states may have consequences for detecting and manipulating MMs at finite temperatures. One of the simplest signatures of an MM is the zero-bias tunneling conductance peak. The voltage resolution of a tunneling conductance measurement, which directly probes the LDOS, is limited by the finite tunneling rate and temperature. Low-energy subgap states as in Fig. 3 and Fig. 4 would contribute to tunneling if the energy of the subgap states is lower than either the temperature or the tunneling-induced broadening. However, since there is a repulsion of these states from zero energy [Fig. 4(a,b)], the likelihood for the states to influence the zero-bias conductance is small unless the temperature is high and the number of channels is large. Thus, the zero-bias effective MM tunneling conductance peak may survive the existence of fermionic subgap states. For utilizing the MM for topological quantum computation, it is known that extra localized states do not affect the phase of manipulation [37]. However, the additional subgap levels could have an influence for the readout schemes that rely on measuring single-particle spectra [38], because this requires eliminating the TR-breaking region to hybridize the two MMs to finite energies. In spite of this, the TI/SC structure has an advantage in regards to robustness against disorder, since disorder cannot degrade the SC gap deep in the SC region thus hybridizing the two MMs at the ends. Also, the potential-fluctuation-induced subgap states show a repulsion from zero energy, without any complications arising from weak antilocalization [22, 39].

Experimentally, the conductance of a TI edge was mea-

sured as $2e^2/h$ [30], which might appear to contradict our assumption of multiple edge channels. However, the simple relation $N_{\rm ch} = \frac{G}{(2e^2/h)}$ between conductance G and the number of channels $N_{\rm ch}$ is valid in the clean limit only. With disorder, the conductance should be analyzed using random matrix theory of the edge transmission matrix [40]. Since the multi-channel TI edge belongs to the symplectic class with odd number of channels, only one channel remains delocalized [41]. A conductance measurement with a length scale greater than the localization length would then produce $G = 2e^2/h$ even if many channels are present. Therefore, the conductance measurement alone cannot rule out the presence of multiple channels.

To conclude, we have studied the effects of multiple channels and disorder near an SC/FI interface on the edge of a 2D TI in the context of MM in the system. We find that a number of localized states, equal to the number of channels, appears at the SC/FI interface. One of these states is the zero-energy MM while the energies of the other states depend on the specific details of the system. Adding disorder in the SC region leads to a distribution in the energies of these extra localized states, potentially reaching the subgap regime. However their effect is less detrimental than those in the SM/SC nanowire structures since they are repelled from zero energy and are localized at the boundary.

This work is supported by JQI-NSF-PFC and Microsoft Q.

Appendix A: Scattering Matrix Approach

In this appendix we present the details of the derivation of zero-energy modes by scattering matrices.

Consider an SC-N-FI problem, such that the interface between SC and FI is expanded to a finite width. A solution in N is

$$\psi^\dagger = u_+\psi_+^\dagger + u_-\psi_-^\dagger + v_-\psi_- + v_+\psi_+, \tag{A1}$$

in which the multi-component $\psi_\pm$ are Kramer's pairs and the subscripts $\pm$ represents right/left moving modes. The corresponding particle-hole-conjugated and time-reversed solutions are:

$$\mathcal{C}\psi^\dagger\mathcal{C}^{-1} = v_+^*\psi_+^\dagger + v_L^*\psi_-^\dagger + u_-^*\psi_- + u_+^*\psi_+ \tag{A2}$$

$$\mathcal{T}\psi^\dagger\mathcal{T}^{-1} = -u_-^*\psi_+^\dagger + u_+^*\psi_-^\dagger + v_+^*\psi_- - v_-^*\psi_+ \tag{A3}$$

Reflection matrices R relates the coefficients of $\left(\psi_+^\dagger, \psi_+\right)$ to those of $\left(\psi_-^\dagger, \psi_-\right)$. At the left (SC/N) interface, the particle-hole symmetry and time-reversal symmetry are both respected, giving three equations for R:

$$\begin{pmatrix} u_+ \\ v_+ \end{pmatrix} = R \begin{pmatrix} u_- \\ v_- \end{pmatrix} \tag{A4}$$

$$\begin{pmatrix} v_+^* \\ u_+^* \end{pmatrix} = R \begin{pmatrix} v_-^* \\ u_-^* \end{pmatrix} \tag{A5}$$

$$\begin{pmatrix} -u_-^* \\ -v_-^* \end{pmatrix} = R \begin{pmatrix} u_+^* \\ v_+^* \end{pmatrix}, \tag{A6}$$

from which one can derive

$$R = \tau_x R^* \tau_x = -R^T. \tag{A7}$$

Together with the unitarity condition $R^\dagger R = 1$, the value of $\det R$ could be computed. First note that the constraint $R = \tau_x R^* \tau_x$ requires R to take the form $R = \begin{pmatrix} r_{ee} & r_{eh} \\ r_{eh}^* & r_{ee}^* \end{pmatrix}$, while the condition $R = -R^T$ implies that r_{ee} is antisymmetric, and, since its dimension is odd, it is singular. Since R itself is non-singular (by the unitarity condition), this implies that r_{eh} is invertible. The remaining conditions $R^\dagger R = 1$ implies

$$r_{eh}^\dagger r_{ee} + r_{ee}^T r_{eh}^* = 0 \Rightarrow r_{ee} r_{eh}^{*-1} = -r_{eh}^{\dagger-1} r_{ee}^T \tag{A8}$$

$$r_{eh}^\dagger r_{eh} + r_{ee}^T r_{ee}^* = 1 \Rightarrow r_{ee}^T r_{ee}^* = 1 - r_{eh}^\dagger r_{eh} \tag{A9}$$

$$\tag{A10}$$

Now we evaluate $\det R$:

$$\begin{aligned} \det R &= (-1)^{N_{\rm ch}} \det \begin{pmatrix} r_{eh} & r_{ee} \\ r_{ee}^* & r_{eh}^* \end{pmatrix} \\ &= (-1)^{N_{\rm ch}} \det \left(r_{eh}^* r_{eh} - r_{eh}^* r_{ee} r_{eh}^{*-1} r_{ee}^* \right) \\ &= -\det \left(r_{eh}^* r_{eh}^{\dagger-1} \right) \qquad \text{(A11)} \\ &= -1 \qquad \text{(A12)} \end{aligned}$$

where we have utilized the fact that r_{eh} is invertible and Eqs. (A8, A9) are consecutively used in the intermediate steps. $N_{\rm ch} = \dim R/2$ is the number of channels in the model, which is restricted to be odd due to the nature of the topological insulator edge.

At the right (N/FI) interface we have no Andreev reflection or time-reversal symmetry, constraining the form of $\tilde{R}$ to be $\tilde{R} = \begin{pmatrix} \tilde{r}_{ee} & 0 \\ 0 & \tilde{r}_{ee}^* \end{pmatrix}$. By the unitarity of $\tilde{R}$, we have $\det \tilde{R} = 1$.

The zero-energy modes are found by solving $\det\left(1 - \tilde{R}R\right) = 0$, which implies that the multiplicity of the eigenvalue -1 of $-\tilde{R}R$ gives the number of zero-energy modes. We now prove that $-\tilde{R}R$ must have at least one eigenvalue being -1. To this end we rotate R to the Majorana basis via $\Omega = \frac{1}{\sqrt{2}} \begin{pmatrix} 1 & 1 \\ -i & i \end{pmatrix}$:

$$\Omega R \Omega^\dagger = 2 \begin{bmatrix} \mathrm{Re}\,(r_{ee} + r_{eh}) & -\mathrm{Im}\,(r_{ee} - r_{eh}) \\ \mathrm{Im}\,(r_{ee} - r_{eh}) & \mathrm{Re}\,(r_{ee} - r_{eh}) \end{bmatrix} \tag{A13}$$

This matrix is real and, because it is unitary, it is also orthogonal. Similarly for $\tilde{R}$ and hence $-\tilde{R}R$. The eigenvalues of an orthogonal matrix can only be 1, -1, or pairs of conjugate $e^{\pm i\phi}$. Since $\det\left(-\tilde{R}R\right) = -1$, $-\tilde{R}R$ must have *at least* one eigenvalue being -1. On the other hand, because there are no other constraints on the problem, there could be *at most* $N_{\rm ch}$ eigenvalues being -1, and hence, at most $N_{\rm ch}$ zero modes.

[1] C. W. J. Beenakker, Annu. Rev. Con. Mat. Phys. **4**, 113 (2013).
[2] J. Alicea, Rep. Prog. Phys. **75**, 076501 (2012).
[3] M. Leijnse and K. Flensberg, Semicond. Sci. Technol. **27**, 124003 (2012).
[4] T. D. Stanescu and S. Tewari, J. Phys. Condens. Matter **25**, 233201 (2013).
[5] V. Mourik, K. Zuo, S. M. Frolov, S. R. Plissard, E. P. A. M. Bakkers, and L. P. Kouwenhoven, Science **336**, 1003 (2012).
[6] M. T. Deng, C. L. Yu, G. Y. Huang, M. Larsson, P. Caroff, and H. Q. Xu, Nano Lett. **12**, 6414 (2012).
[7] A. Das, Y. Ronen, Y. Most, Y. Oreg, M. Heiblum, and H. Shtrikman, Nat. Phys. **8**, 887 (2012).
[8] H. O. H. Churchill, V. Fatemi, K. Grove-Rasmussen, M. T. Deng, P. Caroff, H. Q. Xu, and C. M. Marcus, Phys. Rev. B **87**, 241401 (2013).
[9] A. D. K. Finck, D. J. Van Harlingen, P. K. Mohseni, K. Jung, and X. Li, Phys. Rev. Lett. **110**, 126406 (2013).
[10] L. P. Rokhinson, X. Liu, and J. K. Furdyna, Nat. Phys. **8**, 795 (2012).
[11] R. M. Lutchyn, J. D. Sau, and S. Das Sarma, Phys. Rev. Lett. **105**, 077001 (2010).
[12] J. D. Sau, S. Tewari, R. M. Lutchyn, T. D. Stanescu, and S. Das Sarma, Phys. Rev. B **82**, 214509 (2010).
[13] Y. Oreg, G. Refael, and F. von Oppen, Phys. Rev. Lett. **105**, 177002 (2010).
[14] J. R. Williams, A. J. Bestwick, P. Gallagher, S. S. Hong, Y. Cui, A. S. Bleich, J. G. Analytis, I. R. Fisher, and D. Goldhaber-Gordon, Phys. Rev. Lett. **109**, 056803 (2012); I. Knez, R.-R. Du, and G. Sullivan, Phys. Rev. Lett. **107**, 136603 (2011); Phys. Rev. Lett. **109**, 186603 (2012); F. Qu, F. Yang, J. Shen, Y. Ding, J. Chen, Z. Ji, G. Liu, J. Fan, X. Jing, C. Yang, *et al.*, Sci. Rep. **2**, 339 (2012); L. Du, I. Knez, G. Sullivan, and R.-R. Du, arXiv:1306.1925 (2013); J. B. Oostinga, L. Maier, P. Schüffelgen, D. Knott, C. Ames, C. Brüne, G. Tkachov, H. Buhmann, and L. W. Molenkamp, Phys. Rev. X **3**, 021007 (2013); C. Kurter, A. D. Finck, Y. S. Hor, and D. J. Van Harlingen, arXiv:1307.7764 (2013); V. Orlyanchik, M. P. Stehno, C. D. Nugroho, P. Ghaemi, M. Brahlek, N. Koirala, S. Oh, and D. J. Van Harlingen, arXiv:1309.0163 (2013); J.-P. Xu, M.-X. Wang, Z. L. Liu, J.-F. Ge, X. Yang, C. Liu, Z. A. Xu, D. Guan, C. L. Gao, D. Qian, *et al.*, arXiv:1312.7110 (2013); S. Hart, H. Ren, T. Wagner, P. Leubner, M. Mühlbauer, C. Brüne, H. Buhmann, L. W. Molenkamp, and A. Yacoby, Nat. Phys. **10**, 638 (2014); V. S. Pribiag, A. J. Beukman, F. Qu, M. C. Cassidy, C. Charpentier, W. Wegscheider, and L. P. Kouwenhoven, arXiv:1408.1701 (2014).
[15] L. Fu and C. L. Kane, Phys. Rev. Lett. **100**, 096407 (2008).
[16] L. Fu and C. L. Kane, Phys. Rev. B **79**, 161408 (2009); Phys. Rev. Lett. **102**, 216403 (2009).
[17] A. R. Akhmerov, J. Nilsson, and C. W. J. Beenakker, Phys. Rev. Lett. **102**, 216404 (2009); J. Linder, Y. Tanaka, T. Yokoyama, A. Sudbø, and N. Nagaosa, Phys. Rev. Lett. **104**, 067001 (2010); C. Xu and L. Fu, Phys. Rev. B **81**, 134435 (2010); A. Cook and M. Franz, Phys. Rev. B **84**, 201105 (2011); S. Mi, D. I. Pikulin, M. Wimmer, and C. W. J. Beenakker, Phys. Rev. B **87**, 241405 (2013).
[18] J. D. Sau, R. M. Lutchyn, S. Tewari, and S. Das Sarma, Phys. Rev. Lett. **104**, 040502 (2010).
[19] T. D. Stanescu, R. M. Lutchyn, and S. Das Sarma, Phys. Rev. B **84**, 144522 (2011).
[20] A. R. Akhmerov, J. P. Dahlhaus, F. Hassler, M. Wimmer, and C. W. J. Beenakker, Phys. Rev. Lett. **106**, 057001 (2011).
[21] F. Pientka, G. Kells, A. Romito, P. W. Brouwer, and F. von Oppen, Phys. Rev. Lett. **109**, 227006 (2012); J. D. Sau, S. Tewari, and S. Das Sarma, Phys. Rev. B **85**, 064512 (2012); P. W. Brouwer, M. Duckheim, A. Romito, and F. von Oppen, Phys. Rev. B **84**, 144526 (2011); P. Neven, D. Bagrets, and A. Altland, New J. Phys. **15**, 055019 (2013); I. Adagideli, M. Wimmer, and A. Teker, arXiv:1302.2612 (2013).
[22] D. I. Pikulin, J. P. Dahlhaus, M. Wimmer, H. Schomerus, and C. W. J. Beenakker, New J. Phys. **14**, 125011 (2012).
[23] A. C. Potter and P. A. Lee, Phys. Rev. B **83**, 184520 (2011).
[24] P. Anderson, J. Phys. Chem. Solids **11**, 26 (1959).
[25] G. Tkachov, Phys. Rev. B **87**, 245422 (2013).
[26] J. I. Väyrynen, M. Goldstein, and L. I. Glazman, Phys. Rev. Lett. **110**, 216402 (2013).
[27] M. Bianchi, D. Guan, S. Bao, J. Mi, B. B. Iversen, P. D. C. King, and P. Hofmann, Nat. Commun. **1**, 128 (2010).
[28] M. S. Bahramy, P. D. C. King, A. De La Torre, J. Chang, M. Shi, L. Patthey, G. Balakrishnan, P. Hofmann,

R. Arita, N. Nagaosa, and F. Baumberger, Nat. Commun. **3**, 1159 (2012).
[29] B. A. Bernevig, T. L. Hughes, and S.-C. Zhang, Science **314**, 1757 (2006).
[30] M. König, S. Wiedmann, C. Brüne, A. Roth, H. Buhmann, L. W. Molenkamp, X.-L. Qi, and S.-C. Zhang, Science **318**, 766 (2007).
[31] C. Kittel, *Introduction to Solid State Physics* (John Wiley and Sons, New York, 1986).
[32] S. Takei, B. M. Fregoso, H.-Y. Hui, A. M. Lobos, and S. Das Sarma, Phys. Rev. Lett. **110**, 186803 (2013).
[33] M. Wimmer, A. R. Akhmerov, J. P. Dahlhaus, and C. W. J. Beenakker, New J. Phys. **13**, 053016 (2011).
[34] P. G. de Gennes, *Superconductivty of Metals and Alloys* (Addison-Wesley, Reading MA, 1989); F. Gygi and M. Schluter, Phys. Rev. B **41**, 822 (1990).
[35] D. A. Ivanov, Journal of Mathematical Physics **43**, 126 (2002); D. Bagrets and A. Altland, Phys. Rev. Lett. **109**, 227005 (2012); P. A. Ioselevich, P. M. Ostrovsky, and M. V. Feigel'man, Phys. Rev. B **86**, 035441 (2012).
[36] T. D. Stanescu, R. M. Lutchyn, and S. Das Sarma, Phys. Rev. B **90**, 085302 (2014).
[37] A. R. Akhmerov, Phys. Rev. B **82**, 020509 (2010).
[38] K. Flensberg, Phys. Rev. Lett. **106**, 090503 (2011).
[39] J. D. Sau and S. Das Sarma, Phys. Rev. B **88**, 064506 (2013).
[40] C. W. J. Beenakker, Rev. Mod. Phys. **69**, 731 (1997).
[41] Y. Takane, J. Phys. Soc. Jpn. **73**, 2366 (2004).